Journal of Chromatography A, 1217 (2010) 199–208

Contents lists available at ScienceDirect

Journal of Chromatography A

journal homepage: www.elsevier.com/locate/chroma

A new thermodynamic model describes the effects of ligand density and type, salt concentration and protein species in hydrophobic interaction chromatography

R.W. Deitcher, J.E. Rome, P.A. Gildea, J.P. O'Connell, E.J. Fernandez *

Department of Chemical Engineering, University of Virginia, Charlottesville, VA 22904-4741, USA

ARTICLE INFO

Article history:
Available online 3 August 2009

Keywords:
Retention model
Protein adsorption thermodynamics
Ligand density
Protein adsorption isotherm

ABSTRACT

A new thermodynamic model is derived that describes both loading and pulse-response behavior of proteins in hydrophobic interaction chromatography (HIC). The model describes adsorption in terms of protein and solvent activities, and water displacement from hydrophobic interfaces, and distinguishes contributions from ligand density, ligand type and protein species. Experimental isocratic response and loading data for a set of globular proteins on Sepharose™ resins of various ligand types and densities are described by the model with a limited number of parameters. The model is explicit in ligand density and may provide insight into the sensitivity of protein retention to ligand density in HIC as well as the limited reproducibility of HIC data.

1. Introduction

Hydrophobic interaction chromatography (HIC) continues to be an important technique used in the purification of biological macromolecules [1–8]; however, the relationships between many process variables and the observed chromatographic behavior are poorly understood. Process design and optimization is usually achieved through exhaustive experimentation, and substantial work has been conducted to develop high-throughput experimental methods to facilitate the screening of a large process design space [9,10]. Design efforts would be greatly aided by a model that enables the reduction of the design space based on a fundamental understanding of the thermodynamics of HIC retention.

There have been considerable efforts toward theoretical understanding of the mechanism of protein retention on hydrophobic chromatography surfaces [11–14]. The solvophobic theory [15], based on the association and solvation of the participating species, describes retention in terms of the molal surface tension increment of the salt [16,17]. Fausnaugh and Regnier [18] studied the HIC adsorption of several proteins in the presence of different types of salts and found that the solvophobic theory alone could not adequately explain retention differences.

The preferential interaction theory [19] has been successfully applied to the description of salt effects in HIC retention [20–22]. In this model, the effect of salt concentration in the mobile phase is related to the number of interfacial water molecules and salt ions that are displaced to the bulk solution upon protein adsorption. However, the derivation of the governing equation results in an integrating constant that is independent of salt concentration and is not related to any physical system attributes, but is required to describe the behavior of adsorption systems. Further, the model includes a logarithmic dependence on salt concentration that diverges in the limit of no salt in the mobile phase, and the model cannot be extended to describe the effects of protein loading.

A different approach to modeling salt effects in protein HIC was taken by Chen and Sun [23], who describe a "desolvation" of hydrophobic patches on the protein surface and hydrophobic resin ligands by salt ions, followed by adsorption of the dehydrated protein to the dehydrated ligands. The model improved upon previous efforts by explicitly accounting for ligand density and protein loading effects. However, the model was applied to only a single protein species and ligand type, so that the relationship between model parameters and the properties of the protein and ligand are not clear. Additionally, the model was applied only to isotherm data, and the model derivation results in a predicted log–log relationship between the chromatographic retention factor and salt concentration that is generally inconsistent with experimental observation.

Recently, the thermodynamic treatment of Mollerup [24–26] addressed the effects of mobile phase salt concentration, ligand density, and protein loading effects. Interestingly, the theory suggested that the change in adsorption strength with changes in salt concentration is governed only by the protein species and salt type, and thus is independent of resin properties. Experimental evidence

* Corresponding author. Tel.: +1 434 924 1351.
E-mail address: ejf3c@virginia.edu (E.J. Fernandez).

0021-9673/$ – see front matter © 2009 Elsevier B.V. All rights reserved.
doi:10.1016/j.chroma.2009.07.068

was cited to support this result [27], but this is inconsistent with other HIC data [20,21].

In this paper, we build upon previous efforts and propose a new thermodynamic model of protein retention in HIC. The proposed model includes water as a participant in the adsorption process and utilizes activity models to describe the influence of salt on retention. The developed isotherm model is parameterized using isocratic elution chromatography (IEC) and adsorption isotherm data. Further, we compare the results of the experimental studies with recently published results to investigate the reproducibility of measured retention in HIC systems, and interpret the reproducibility in the context of the currently proposed model.

2. Theory

The adsorption of a protein to a HIC surface has been modeled as the interaction of a protein molecule with a stoichiometric number of ligands to form a protein–ligand complex [20,24–26]:

$$P_{sol} + \nu L \Leftrightarrow P_{ads}.$$

In such a model, solvent and salt ions in solution do not appear explicitly, but are accounted for in the model equations by their effects on the properties of the participating species [24–26] or stoichiometric relationships with the protein and ligand [20].

In the currently proposed model, we include solvent (water) molecules as explicit participants in the adsorption process. Displacement of water molecules from hydrophobic surfaces is included as follows:

$$P_{sol} + \nu L \Leftrightarrow P_{ads} + \nu\xi W.$$

The stoichiometric coefficient ξ corresponds to the number of water molecules released from the protein and ligand per protein–ligand contact, and will be characteristic of the ligand type. The description of HIC as a water displacement process was originally proposed by Geng and co-workers [28]. This model differs from that of Sun and Chen [23], since salt ions do not participate in the reaction. Rather, the role of salt is to affect the thermodynamic properties of species in the mobile phase, as will be described below.

In deriving the fundamental relationships describing the thermodynamics of protein adsorption, we follow closely the approach recently demonstrated by Mollerup [24–26]. Based on the proposed model, the equilibrium constant for protein adsorption is expressed in terms of the activities of the participating species,

$$K = \frac{a_{P_{ads}} a_W^{\nu\xi}}{a_{P_{sol}} a_L^{\nu}} = \frac{(x_{P_{ads}}\gamma_{P_{ads}})a_W^{\nu\xi}}{(x_{P_{sol}}\gamma_{P_{sol}})(x_L\gamma_L)^{\nu}} \cong \frac{q_P\gamma_{P_{ads}}c^{\nu}}{c_P\gamma_{P_{sol}}c_L^{\nu}} a_W^{\nu\xi}. \quad (1)$$

Here, the activities of adsorbed protein, solution-phase protein and ligand are described as the product of activity coefficients and fractional concentrations, and the ligand has been approximated as an ideal species with $\gamma = 1$, consistent with the analysis of Mollerup [25]. The fractional concentrations of species in both the stationary and mobile phases are based on a common value for the total concentration of species, c.

The dependence of the activity coefficient of hydrated protein on salt concentration is modeled in the following way,

$$\ln\gamma_{P_{sol}} = \ln\gamma_{P_{sol}}^{\infty} + \kappa_{salt}c_{salt} + \kappa_P c_P \cong \ln\gamma_{P_{sol}}^{\infty} + \kappa_{salt}c_{salt}. \quad (2)$$

The assumption that $\kappa_{salt}c_{salt} \gg \kappa_P c_P$ is based on the analysis of lysozyme HIC retention and solubility data by Mollerup [24], in which κ_{salt} was determined to be approximately two orders of magnitude smaller than κ_P, while in all of the experimental conditions explored in this work, c_{salt} is approximately four orders of magnitude larger than c_P.

The adsorbed protein activity coefficient is assumed to be independent of mobile phase salt concentration, but lateral interactions between adsorbed proteins are included with an empirical relation having a loading dependence suggested in the literature [29],

$$\ln\gamma_{P_{ads}} = \ln\gamma_{P_{ads}}^{\infty} + \ln(1 + \varepsilon q_P). \quad (3)$$

Finally, the thermodynamic activity of water in electrolyte solutions has been well studied, with theoretical models and tabulated data available in the literature [30,31]. For many salts and concentrations of practical interest in HIC, however, we propose that a simple linear empirical model is sufficient:

$$\ln a_W = \rho c_{salt}. \quad (4)$$

Defining the free ligand concentration as a function of the ligand density, protein–ligand stoichiometry and loading,

$$c_L = \Lambda - \nu q_P, \quad (5)$$

and substituting Eqs. (2), (3), (4) and (5) into Eq. (1) yields the following isotherm model,

$$\ln K = \ln\left(\frac{q_P}{c_P}\right) + (\ln\gamma_{P_{ads}}^{\infty} + \ln(1 + \varepsilon q_P)) - (\ln\gamma_{P_{sol}}^{\infty} + \kappa_{salt}c_{salt}) + \nu\ln\left(\frac{c}{\Lambda - \nu q_P}\right) + \nu\xi\rho c_{salt}. \quad (6)$$

The partition coefficient is defined in the following way,

$$\ln A \equiv \lim_{c_P\to 0}\ln\left(\frac{\partial q_P}{\partial c_P}\right) = \lim_{c_P\to 0}\ln\left(\frac{q_P}{c_P}\right), \quad (7)$$

and, taking the appropriate limit of Eq. (6) and with some algebraic rearrangement,

$$\ln A = \left(\ln K + \nu\ln\left(\frac{\Lambda}{c}\right) + \ln\left(\frac{\gamma_{P_{sol}}^{\infty}}{\gamma_{P_{ads}}^{\infty}}\right)\right) + (\kappa_{salt} - \nu\xi\rho)c_{salt}. \quad (8)$$

The partition coefficient is related to the retention factor observed in pulse-response chromatography,

$$\ln A = \ln k' - \ln\phi. \quad (9)$$

Here we define the phase ratio as the ratio of solid and mobile phase volumes, and the protein concentration in the adsorbed phase is relative to the volume of stationary phase. The resulting relationship for the retention factor, by substitution of Eq. (9) into Eq. (8), is that the natural logarithm of the retention factor varies linearly with salt concentration, consistent with literature data for HIC at high salt conditions [17,18,32]. For simplification purposes, we define the following groupings of model parameters:

$$\alpha \equiv \left(\ln K + \nu\ln\left(\frac{\Lambda}{c}\right) + \ln\left(\frac{\gamma_{P_{sol}}^{\infty}}{\gamma_{P_{ads}}^{\infty}}\right)\right) + \ln\phi \quad (10)$$

$$\beta \equiv \kappa_{salt} - \nu\xi\rho, \quad (11)$$

so that an appropriate expression of the retention factor is

$$\ln k' = \alpha + \beta c_{salt}. \quad (12)$$

Substitution of Eqs. (8) and (9) into Eq. (6) allows the isotherm model to be expressed in terms of the retention factor and phase ratio,

$$\ln\left(\frac{q_P}{c_P}\right) = \ln k' - \ln\phi + \nu\ln\left(1 - \frac{\nu q_P}{\Lambda}\right) - \ln(1 + \varepsilon q_P). \quad (13)$$

Several assumptions and approximations have been used in the development of this model and the governing equations. The model neglects interactions between the protein and the base matrix of the resin, and may therefore not be appropriate for HIC resins in which the base matrix has some hydrophobic character and contributes to

the protein–resin interaction. The model formulation also assumes that salt ions are preferentially excluded from the hydrophobic interfaces on the protein and resin surfaces, so that the displacement of salt ions is not included in the model. This assumption, along with the linear dependence of the hydrated protein activity coefficient on salt concentration, results in a model that does not describe the weakening effect of salt on retention observed experimentally at very low salt concentrations [14,20,22,27]. This "salting in" behavior might be captured by including a Debye–Huckel term in the protein activity coefficient model; however, the aim of this work is to describe protein adsorption in HIC under strongly retaining conditions where "salting out" behavior is dominant. In addition to these assumptions, empirical relations are employed extensively, for the purposes of simplifying the mathematics or to describe thermodynamics for which there is at present a lack of theoretical understanding.

3. Materials and methods

3.1. Materials

Proteins utilized in this study were purchased from Sigma–Aldrich (St. Louis, MO, USA). The proteins investigated are: α-lactalbumin (bovine), ribonuclease A (bovine), cytochrome C (equine), ovalbumin (hen egg white), lysozyme (hen egg white) and carbonic anhydrase (bovine). Ammonium sulfate, MOPS, sodium nitrate and calcium chloride were purchased from Fisher Scientific (Houston, TX, USA) and were of HPLC-grade quality or better.

GE Healthcare (Piscataway, NJ, USA) Sepharose™ hydrophobic interaction chromatography resins were purchased from Fisher Scientific (Houston, TX, USA). The resin materials used in this work are: Phenyl Sepharose™ 6 Fast Flow (high substitution) (40 μmol ligand/ml), Phenyl Sepharose™ 6 Fast Flow (low substitution) (20 μmol ligand/ml), Butyl Sepharose™ 4 Fast Flow (50 μmol ligand/ml) and Octyl Sepharose™ Fast Flow (5 μmol ligand/ml). Properties of these materials, including particle size, ligand density and porosity, are provided by the resin manufacturer and have been reported in the literature [20,21].

3.2. Isocratic elution chromatography

Pulse-response isocratic elution chromatography experiments were performed on an AKTA Explorer chromatography system (GE Healthcare, Piscataway, NJ, USA) using columns prepared by loading resin into HR 5/2 glass shells and flow-packing as per manufacturer recommendations. Bed heights were 2–2.5 cm, and the columns were operated at a flow rate of 0.2 ml/min.

Buffers for the IEC experiments consisted of ammonium sulfate at a specified concentration, 100 mM MOPS, adjusted to pH 7.0. For experiments with α-lactalbumin, 12 mM $CaCl_2$ was included to ensure that the protein was present in the *holo* form. All experiments were conducted at 25 °C.

Chromatography experiments were conducted with the following protocol. First, the column was equilibrated at the salt concentration of interest until a baseline conductivity was established. Protein solution at a concentration of 2.5 mg/ml was loaded onto a 50 μl sample loop, and subsequently loaded onto the column. Effluent from the column was monitored by UV at a wavelength of 280 nm. Upon completion of protein elution as evidenced by the re-establishment of baseline UV absorbance, a step change to zero ammonium sulfate was initiated. Following baseline conductivity and UV absorbance, another step change to 20% ethanol to clean the resin was conducted. Finally, the column was re-equilibrated in MOPS buffer to prepare for the next run.

First moment analysis was applied to the chromatographic peaks to determine the retention volume, and retention factors were calculated with the retention factor definition

$$k' = \frac{\mu - V_0}{V_0}. \tag{14}$$

The unretained volume was measured for each column by pulse injection of sodium nitrate, the column effluent being monitored by UV absorbance at 310 nm.

3.3. Adsorption isotherms

For each isotherm system, the following procedure was followed. A sample of resin slurry was exchanged from the 20% ethanol packing solution to distilled water, then equilibrated to the buffer composition of interest by serial dilutions, to a final resin composition of 50% (v/v) settled bed. Protein solutions were prepared by dissolving the purchased protein in adsorption buffer to a targeted concentration of 7–15 mg/ml. The UV absorbance of a diluted sam-

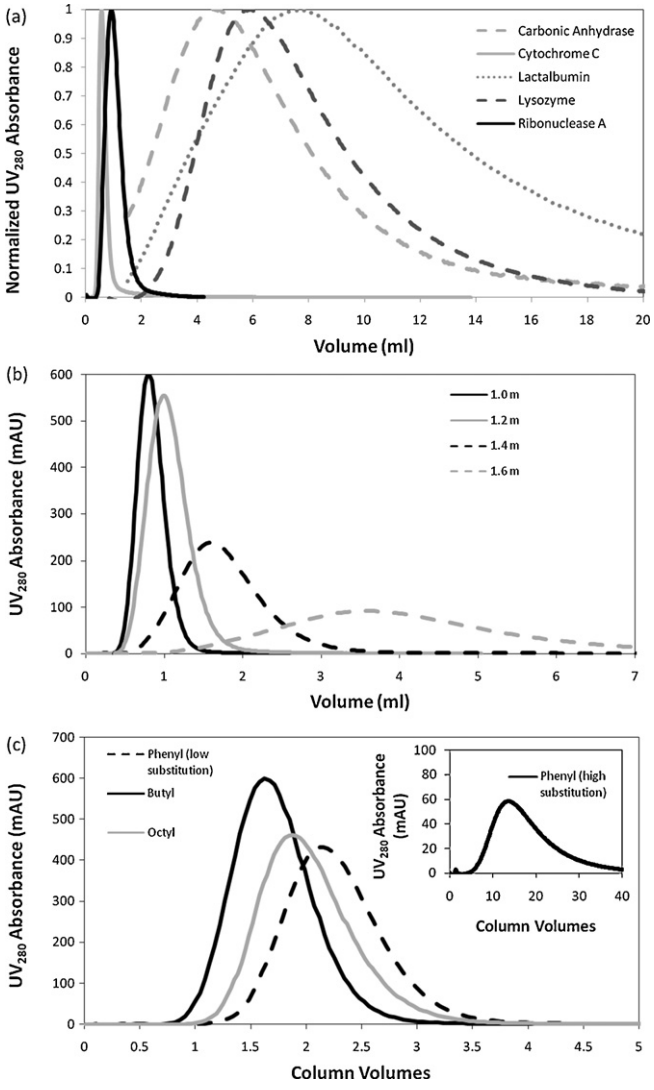

Fig. 1. Effects of protein species and ammonium sulfate concentration on isocratic elution chromatograms. (a) Normalized UV_{280} intensity vs. elution volume for proteins on Phenyl Sepharose™ 6 Fast Flow (high substitution) resin with 1.0 m ammonium sulfate in the mobile phase. (b) UV_{280} intensity vs. elution volume for lysozyme on Butyl Sepharose™ 4 Fast Flow at various ammonium sulfate concentrations. (c) UV_{280} intensity vs. elution column volumes for lysozyme on each Sepharose™ resin studied.

ple of the protein solution was measured at 280 nm. Resin slurry, adsorption buffer and protein solution were combined in varying proportions to a total of 0.5 ml each in 1.5 ml microcentrifuge tubes. Each sample was equilibrated at 25 °C for at least 12 h with rotary agitation. Following equilibration, the samples were settled by microcentrifugation at 8000 RPM for two minutes on an Eppendorf (Hamburg, Germany) 5415 D microcentrifuge. Supernatant was loaded onto an acrylic 96-well plate manufactured by Costar (Corning, NY, USA) and diluted with buffer to obtain protein concentrations in the Beer's law regime. UV absorbance at 280 nm was measured with a Molecular Devices (Sunnyvale, CA, USA) SPECTRAmax 384 Plus plate reader, and converted to protein concentrations utilizing Beer's law and experimentally measured extinction coefficients for each protein. The amount of adsorbed protein was then computed by material balance.

4. Results and discussion

4.1. Isocratic pulse-response results and modeling

The variables explored by isocratic elution chromatography are the protein species, resin type, and ammonium sulfate concentration. Examples of how the observed chromatograms are affected by these variables are shown in Fig. 1. In all cases, single peak behavior was observed, and the peaks became broader as the salt concentration increased. However, the shape of the peaks was affected by each of the variables studied. In particular, the proteins α-lactalbumin, ovalbumin and carbonic anhydrase tended to show increased tailing with increased salt concentration and resin ligand density. An example of this phenomenon is illustrated by Fig. 1(a), as α-lactalbumin begins eluting prior to lysozyme, but elutes over a greater volume. This may be a result of reversible adsorbed protein unfolding; conformation change of α-lactalbumin adsorbed to HIC resins is well-documented [33–35] and has been used to account for asymmetric peak shapes [36,37].

Eq. (12) shows that for each of the protein–resin systems, the natural logarithm of the retention factor should vary linearly with salt concentration. The data collected here, plotted in Fig. 2, are well-described by this relationship, evidenced by correlation coefficients of $R^2 \geq 0.96$ for all systems except cytochrome C on low-substitution phenyl resin, a system where the measured retention was very weak even at high salt concentrations. The six model proteins considered in this work were investigated on all four Sepharose™ resins, with the exception of cytochrome C on Butyl Sepharose™ 4 Fast Flow, a system for which no measurable retention occurred for ammonium sulfate concentrations less than or equal to 2.0 m.

Each protein–resin system is characterized by unique values of α and β, depicted in Fig. 3. Some trends are immediately evident in the data with regard to the resin properties and the β value. Comparison

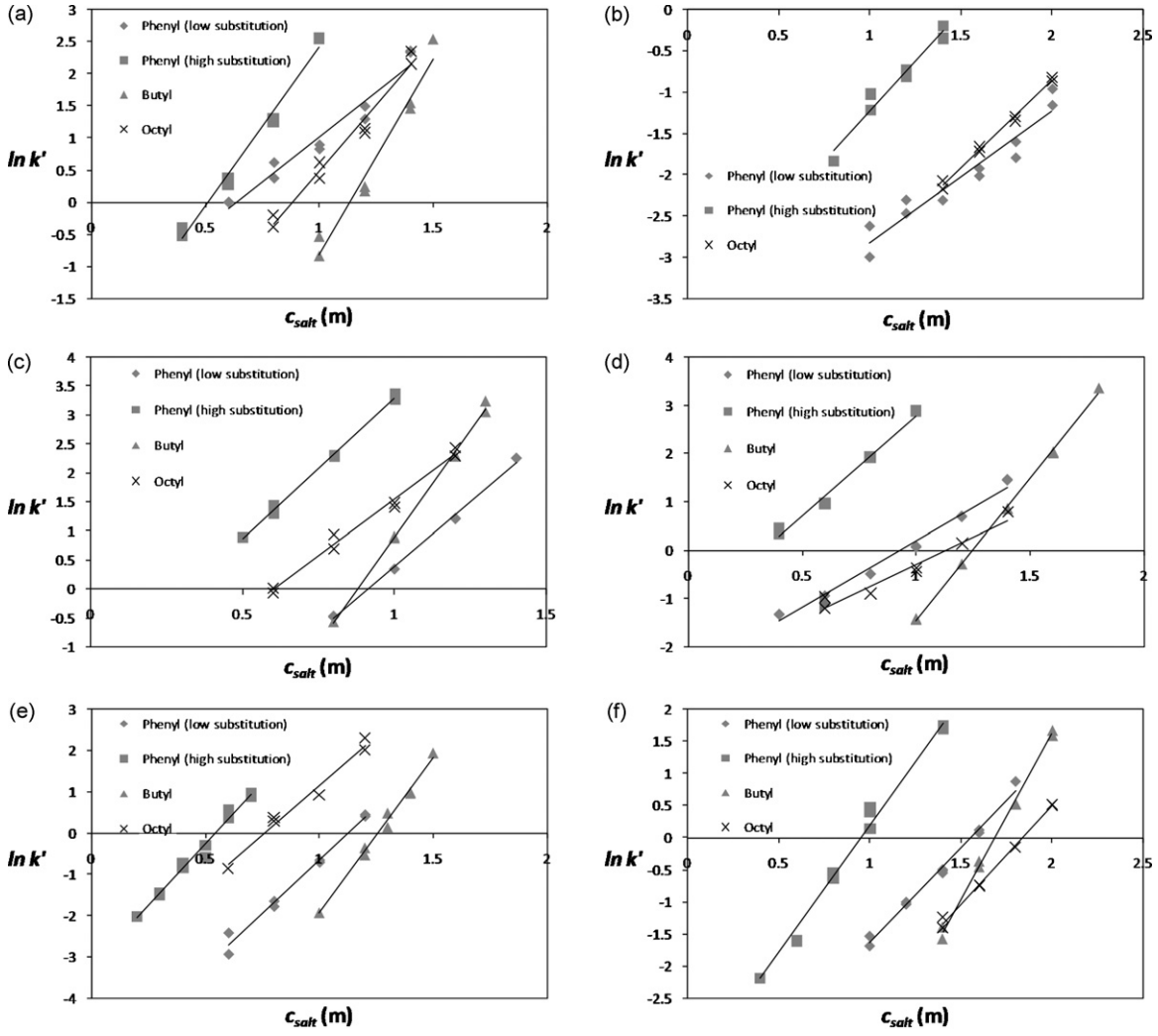

Fig. 2. IEC retention factors plotted against ammonium sulfate concentration: (a) carbonic anhydrase, (b) cytochrome C, (c) α-lactalbumin, (d) lysozyme, (e) ovalbumin and (f) ribonuclease A. Solid lines are the fit of Eq. (11).

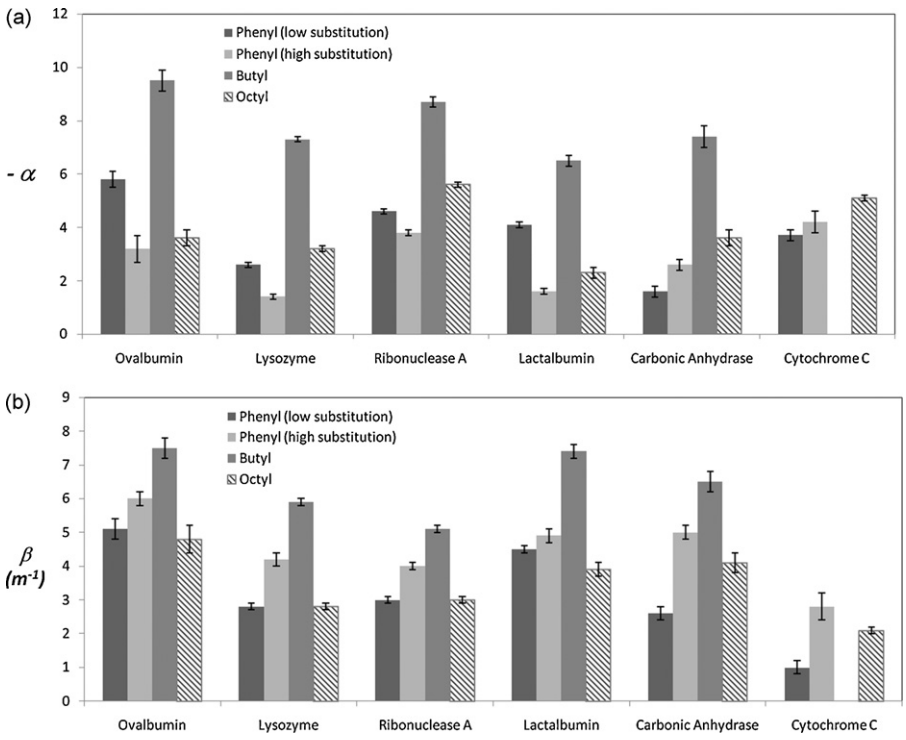

Fig. 3. (a) α and (b) β parameters for the systems studied by IEC.

of the data for the low and high substitution phenyl resins shows that β increases with increased ligand density for all of the proteins studied. Further, the high density butyl resin (40 μmol ligand/ml resin) results in β values that are larger than those of the lower density octyl resin (5 μmol ligand/ml resin) in all cases, despite the shorter alkyl chain length. The salt-dependence observed for many proteins on the low-substitution phenyl and octyl resins are not significantly different, suggesting a compensation between ligand density and ligand type. With regard to the α parameter, increased phenyl ligand density results in an increase in α for each protein except carbonic anhydrase, while the value of α for the butyl resin is substantially lower than that of the other resins in all cases. The cause of the unique relationship between phenyl ligand density and α for carbonic anhydrase is unclear and requires further investigation.

With the value of the binary parameter ν determined by fitting the model to isotherm data (presented in Section 4.2), the IEC retention data were regressed to determine the physically based model parameters. The unknown parameters in Eq. (11), κ_{salt} and ξ, are attributed to the effect of protein species and ligand type, respectively, in the model derivation. However, the undetermined model parameters in Eq. (10) are complex, particularly the standard state equilibrium constant K and the adsorbed protein activity coefficient at infinite dilution, ${\gamma_{Pads}}^{\infty}$, involving interaction between the protein and resin. It is desirable to regress the data without the use of binary parameters, and we propose the following expression,

$$\ln K + \ln\left(\frac{\gamma^{\infty}_{P_{sol}}}{\gamma^{\infty}_{P_{ads}}}\right) = \alpha_{protein} + \nu\alpha_{ligand}, \tag{15}$$

so that the retention data can be fully described in terms of independent contributions from the protein species and resin.

Eqs. (10), (11) and (12) were applied to fit the IEC data by performing a non-linear least-squares regression, and the resulting values of the parameters are presented in Tables 1 and 2. We note that the values reported in Table 1 are determined by the ligand species, and the values tabulated for the phenyl ligand apply to both the high and low ligand density resins. For the ammonium sulfate mobile phase modifier, the value of ρ is 0.35 [31].

Table 1
Ligand-dependent model parameters.

	Phenyl	Butyl	Octyl
ξ	11	16	25
α_{ligand}	13.95	13.10	14.79

Table 1 shows that the value of the parameter α_{ligand} for the three ligand species are similar in value, suggesting that the contribution of ligand properties to the observed α value in protein HIC adsorption may be similar for the ligands considered here. A sensitivity analysis was conducted for the α_{ligand} value for the phenyl ligand, which is observed to be intermediate to the values determined for the butyl and octyl ligands. Changes in the α_{ligand} value of +1% and −1% result in increases in the sum of squared errors (SSE) of 71% and 97%, respectively, when comparing experimentally determined α values with those calculated from the regressed parameters for proteins adsorbed to the phenyl resins. The high sensitivity observed for this parameter indicates that the values of α_{ligand} reported in Table 1 are indicative of a significant influence of the ligand type on the salt-independent adsorption behavior of proteins on these HIC resins.

The values of the stoichiometric number of water molecules, ξ, for the three ligand types can be contrasted with the calculations of Perkins et al. [20], who computed surface areas of these ligands, determining that the butyl ligand (191 Å^2) had a somewhat larger surface area than the phenyl ligand (210 Å^2), while the octyl resin had the most surface area (319 Å^2). It would seem reasonable to expect the ξ value to follow this trend, as more water molecules would be released to the bulk solution with increased protein–ligand contact area, but this is not consistent with our observations. However, we caution against such a literal interpretation of the meaning of the ξ parameter, due to the very simplified model formulation presented here. In particular, we have included water molecules at the ligand interface as part of the hydrated

Table 2
Protein-dependent model parameters.

	Carbonic Anhydrase	Cytochrome C	α-Lactalbumin	Lysozyme	Ovalbumin	Ribonuclease A
κ_{salt} (m^{-1})	2.8	1.1	3.0	2.3	2.9	1.9
$\alpha_{protein}$	1.7	−0.3	2.8	1.8	2.0	0.05

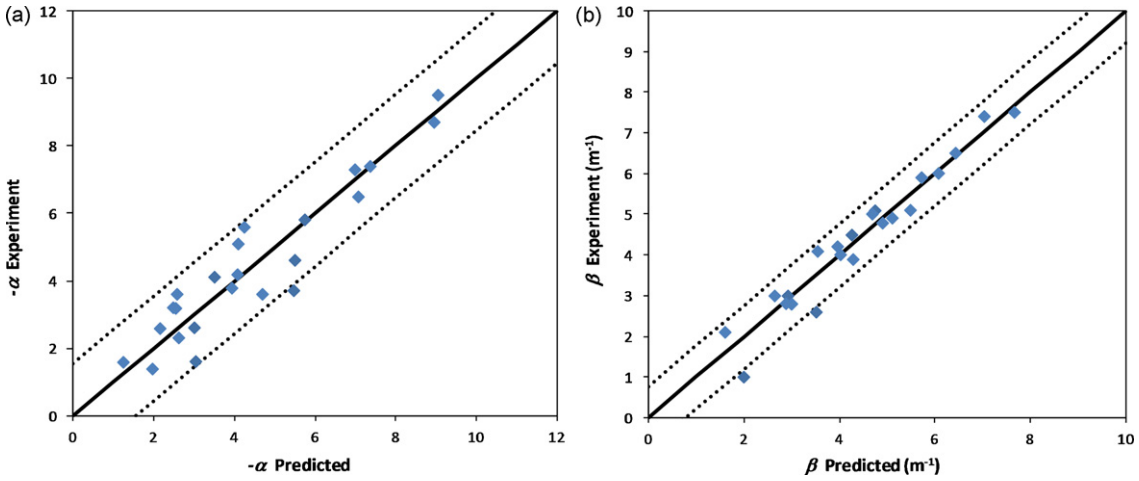

Fig. 4. Correlation of calculated and experimental (a) α and (b) β values. Dashed lines indicate a range of ±2 standard deviations from the solid line $y = x$.

ligand, which is assumed to behave ideally. It has been proposed that aromatic and alkyl hydrocarbons may differ in their effect on the structure of water molecules at the hydrophobic interface [44], so that the energetic difference in water molecules released from these interfaces to the bulk mobile phase would vary by ligand type. Instead, we consider the ξ parameter to be an indicator of the "effective hydrophobicity" of a ligand, related to both the surface area and chemical nature of the ligand type.

The model parameters reported in Table 2 are attributed to the individual protein species in the model derivation. The parameter κ_{salt} appears to increase with molecular weight, except for α-lactalbumin. Such a trend might be expected, based on the physical argument that the effect of salt on protein activity would depend on the surface area available for protein–salt and protein–water interactions. α-Lactalbumin not following this trend might be a result of conformational change during HIC increasing the surface area of the molecule, leading to adsorption behavior expected for a larger molecule. The parameter $\alpha_{protein}$ is less easily interpreted with regard to physical meaning. The model derivation suggests that this parameter is related to the general affinity of a protein for hydrophobic surfaces in the absence of mobile phase modifier. Interestingly, a negative value is determined for cytochrome C, indicating that interactions between this protein and the hydrophobic resins are unfavorable.

Determination of model parameters that are related to the protein species but apply to adsorption behavior on multiple resins, presents a unique opportunity to identify protein macroscopic properties or molecular descriptors that can be universally applied to the prediction of HIC retention. Such protein attributes might be correlated with the protein-dependent model parameters to identify the key properties governing behavior in HIC. However, given the large number of protein attributes that may be considered and the relatively small number of protein species considered here, such an analysis is not feasible with the current data set.

The ability of the model to describe the data is shown graphically by Figs. 4 and 5. Here, values of α and β are calculated using the regressed model parameters in Eqs. (10) and (11). The correlation of experimental and calculated values are quantified by R^2 values of 0.89 for α and 0.95 for β. The high degree of correlation for the β parameter suggests that the majority of the information contained in the data is captured by the model. The greater uncertainty of the α parameter may indicate that the approximation of Eq. (15) neglects specific binary protein–resin interactions that are important in some systems. Correlation of all of the experimental retention data with values calculated from applying the regressed model parameters to Eqs. (10)–(12), as shown in Fig. 5, demonstrate that the general behavior is captured, but scatter in the data is present. These results suggest that the proposed thermodynamic model may be useful as a tool for narrowing the design space for a HIC step, but may not capture sufficient detail for quantitative process optimization.

At this point, we consider evaluation of the proposed model by comparison with other models. Derivation of the model follows closely that of Mollerup [24–26], but the model differs by including the role of solvent molecules in the adsorption process. The most distinct difference in the governing equations is that the salt-dependence of the retention factor, characterized by the β parameter, depends on both the characteristics of the protein and the resin in the proposed model. This result is consistent with the

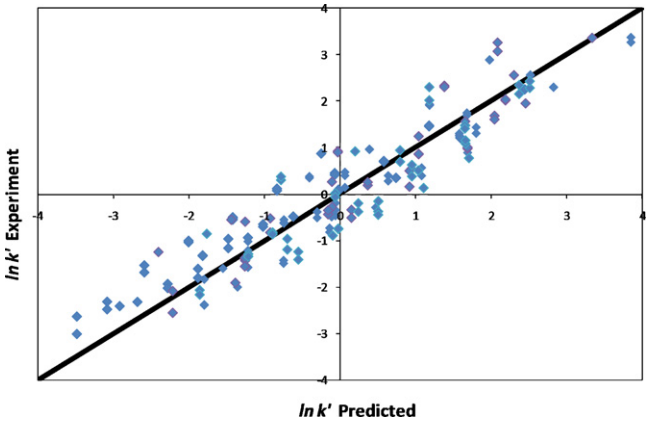

Fig. 5. Correlation of calculated and experimental ln k' values.

data collected in this study, which are not explained by the model of Mollerup.

Conversely, the presently proposed model appears to be inconsistent with the data of Staby and Mollerup [27], where for a single protein species, the same value of β is observed when adsorbed to resins with different ligand types. In that study, however, the POROS resins used are based on a poly(styrene-divinylbenzene) particle matrix, which has been shown to adsorb proteins by hydrophobic interaction even in the absence of functionalization with ligands [45]. It is reasonable to hypothesize that the hydrophobic nature of the base matrix plays a significant role in the adsorption behavior observed by Staby and Mollerup, in which case a model that describes HIC based solely on interactions between proteins and ligands may not be valid.

Parallels between the presently proposed model and the model based on the preferential interaction theory are clear, as each describes the retention in HIC in terms of stoichiometric numbers of water molecules released as a result of protein adsorption. However, the salt-independent term in the preferential interaction theory equation for the retention factor is an integrating constant that is not related to any physical or thermodynamic quantity. In this work, the equivalent salt-independent term has meaningful attributes, creating the possibility to predict values of α for new systems. Additionally, the derivation strategy pursued here applies over a range of protein concentrations, as opposed to the preferential interaction theory, which does not account for loading effects. It is noted that while we have modeled salt as an activity modulator for solvent and solvated protein, an alternate formulation might be to include the release of salt from the protein explicitly,

$$P_{sol} + \nu L \Leftrightarrow P_{ads} + \nu\xi W + \delta S.$$

Experimental evidence indicates that for many salts, including ammonium sulfate, a linear relationship exists between salt concentration and the salt activity [31]. If the above model is used, the definition of the equilibrium constant and subsequent isotherm model would be altered, with the end result that the description of the partition coefficient shown in Eq. (8) would include the additional term $\delta \ln c_{salt}$, equivalent to the preferential interaction model when the salt stoichiometry is independent of salt concentration [20].

4.2. Adsorption isotherm modeling

A favorable result of the derivation strategy followed here is that the fundamental relation derived from the thermodynamic description of protein adsorption is an isotherm model that provides a retention factor model in the limit of low protein concentration. Commonly, HIC batch loading data are described using the Langmuir model, or an exponentially modified Langmuir model [14,38–41]. In the same spirit, we now apply the isotherm model of Eq. (13) to loading data for the same systems investigated by pulse-response chromatography using non-linear, least-squares regression of the isotherm data. An additional advantage is that, utilizing the measured retention factors, the isotherm data for any protein–resin system can be described at multiple salt concentrations using only the fitted parameters ν and ε.

Representative plots of adsorption isotherm data and the corresponding model fits for several protein–resin systems are shown in Fig. 6. The model was applied to isotherm data from Chen and Cramer [42] obtained at 0.8, 1.2 and 1.4 M ammonium sulfate, supplemented with new measurements at ammonium sulfate concentrations of 1.2 and 1.4 M ammonium sulfate. Isotherm measurements were not performed for cytochrome C due to the extremely weak interactions with the HIC resins observed by pulse-response chromatography for this protein.

Application of the derived isotherm model was performed by both including and excluding the term introduced in Eq. (3) to account for lateral interactions of adsorbed proteins. Comparison of the importance of including this term was evaluated by

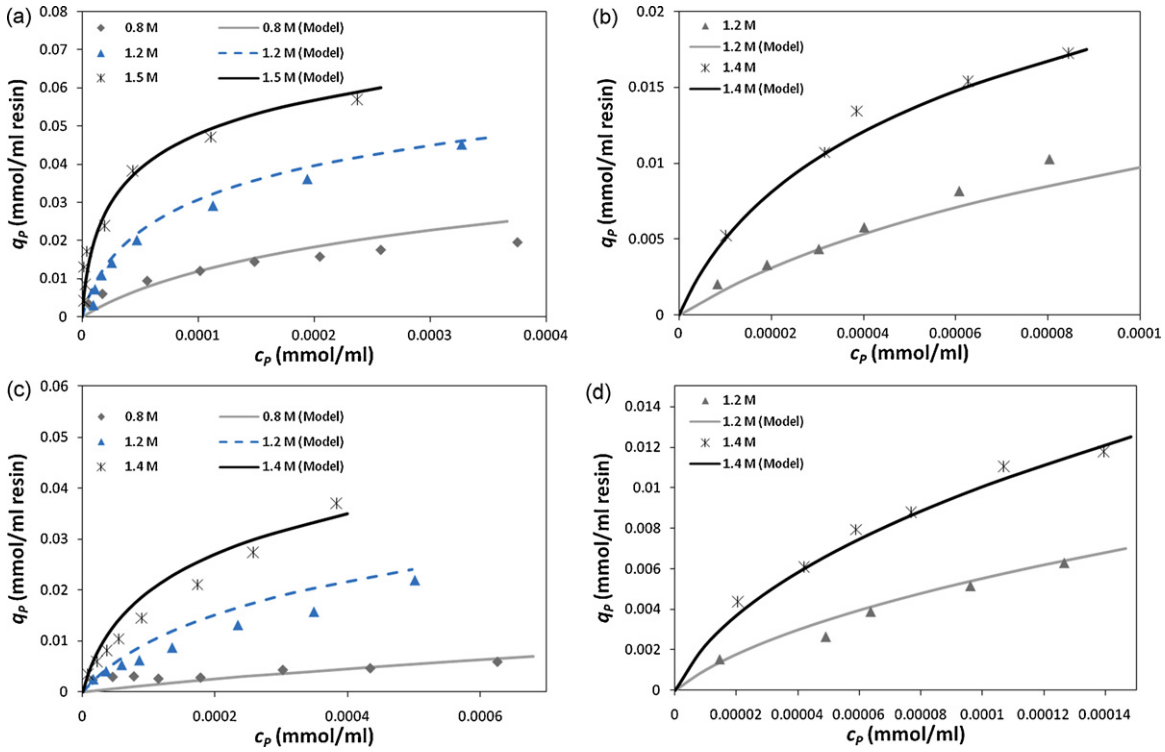

Fig. 6. Adsorption isotherms for (a) α-lactalbumin on Phenyl Sepharose™ 6 Fast Flow (high substitution) resin, (b) ovalbumin on Phenyl Sepharose™ 6 Fast Flow (low substitution), (c) lysozyme on Butyl Sepharose™ 4 Fast Flow resin and (d) carbonic anhydrase on Octyl Sepharose™ 4 Fast Flow resin at the specified ammonium sulfate concentrations. Data in (a) and (c) are from Chen and Cramer [42]. Solid lines are the fit of Eq. (13).

Table 3
Stoichiometric number of ligands contacted per adsorbed protein molecule, ν.

	Phenyl (low substitution)	Phenyl (high substitution)	Butyl	Octyl
Carbonic Anhydrase	2.1	5.6	7.7	1
Lactalbumin	3.9	6.4	8.6	1.8
Lysozyme	2.2	5.1	7.3	1
Ovalbumin	5.6	9.6	10.1	2.7
Ribonuclease A	–	6.3	–	1

performing an *F*-test. For the systems investigated, results of the *F*-test were $P \geq 0.05$, suggesting that lateral interactions do not play a significant role in determining the loading behavior. Based on these results, values for the parameter ε are not reported. However, the range of systems and conditions studied here is limited, and the proposed description of lateral interactions in Eq. (3) is empirical. This result cannot imply that adsorbed protein–protein interactions are generally negligible for protein adsorption systems.

Table 3 lists the values of the binary parameter ν determined for each protein–resin system by fitting isotherm data. Parameter values were limited to a lower bound of $\nu = 1$, so that an adsorbed protein must associate with at least one ligand. For each protein, the ν value increases with increased ligand density, as expected. Values for ribonuclease A adsorbed to the low-substitution phenyl and butyl resins are not reported, as the isocratic elution data indicated that protein adsorption was much weaker than suggested by the initial slopes of the isotherm data, and the regression of Eq. (13) failed to converge. The cause of the discrepancies in these data sets requires further investigation, but we speculate that this result might be attributed to differences in ligand density of the specific resin lots used to obtain the pulse-response and isotherm data (further discussed in Section 4.3).

In order to confirm that the ν values obtained by model fitting are realistic, we compare them with a calculated estimate of the number of ligands a protein would contact upon adsorption from simple, geometric considerations. The hydrodynamic radius of a compact, globular protein can be estimated from the molecular weight [43] by

$$r_H \approx 0.081 MW^{1/3}, \tag{16}$$

where the molecular weight, *MW*, is in Daltons and the computed radius is in nanometers. We then estimate the occupied surface area of an adsorbed protein as that of a circle with a radius equivalent to the hydrodynamic radius of the protein. This leads to an estimate of the average number of ligands per unit surface area of resin based on the nominal ligand density per volume of gel reported by the manufacturer (previously reported [20]) and a literature study of the available surface area of Sepharose™ HIC resins [21]. The resulting equation to estimate the number of ligands contacted per adsorbed protein is

$$\nu_{est} = \pi r_H^2 \Lambda \frac{V_s}{A_s}. \tag{17}$$

Sample data comparing estimated and experimentally determined values of ν are plotted in Fig. 7. In general, the experimentally determined values are similar to the calculated estimates when the number of ligands contacted is low, indicating that the values of ν obtained are physically realistic. For these systems, it may be reasonable to use the rough estimate of ν if experimental isotherm data is not available. For the larger proteins ovalbumin and carbonic anhydrase, calculated contact a large number of ligands upon adsorption, the estimated values are substantially larger than those determined by experiment. This may be a result of over-estimating the occupied surface area of these large molecules upon adsorption, and a more accurate estimate of ν might be obtained by a more sophisticated description of the contact area.

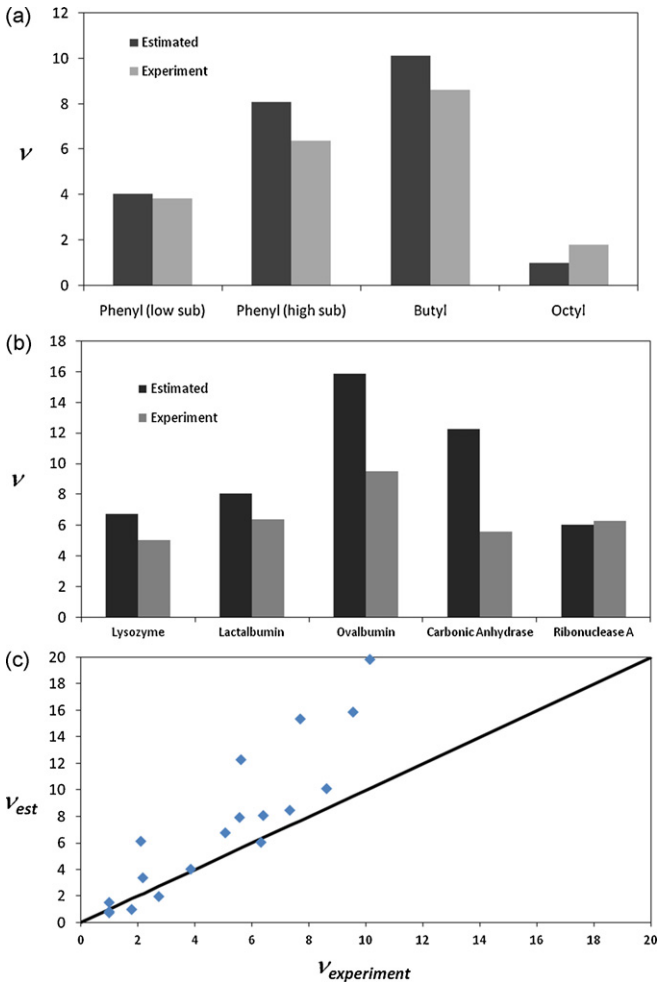

Fig. 7. Comparison of estimated (Eq. (13)) and experimentally determined values of ν for (a) α-lactalbumin adsorbed to several resins, (b) several proteins adsorbed to the Phenyl Sepharose™ 6 Fast Flow (high substitution) resin, and (c) all systems.

4.3. Ligand density sensitivity analysis and HIC reproducibility

A useful aspect of the thermodynamic modeling strategy utilized here, and previously [24–26], is that the ligand density appears

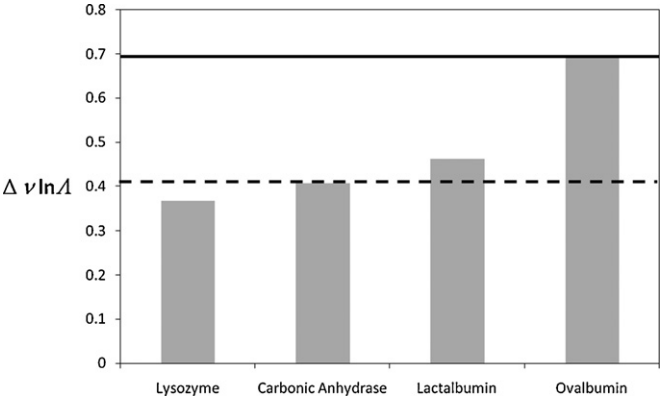

Fig. 8. Calculated change in the term $\nu \ln(\Lambda)$ due to a perturbation of the ligand density of Phenyl Sepharose® (High Substitution) Fast Flow 6 from 40 to 43 μmol/ml for several model proteins. The horizontal lines represent corresponding increases in k' of 50% (dashed) and 100% (solid).

explicitly in the expressions for the isotherm and retention factor. McCue et al. have recently shown that for the purification of a monoclonal antibody from its aggregate, small variations in the ligand density of the Phenyl Sepharose™ 6 Fast Flow (high substitution) resin can significantly impact the binding behavior, as quantified by the Langmuir binding constant [5]. The model proposed in this work may yield some insight into the sensitivity of HIC systems to ligand density.

To investigate this phenomenon, the term $\nu \ln \Lambda$ in Eq. (8) was computed for several of the proteins investigated in this study adsorbed to the high-substitution phenyl resin for ligand densities of 40 and 43 μmol/ml resin. To simplify the analysis, we assume that the number of ligands contacted by an adsorbed protein, ν, is not changed by a small change in the ligand density. The difference in $\nu \ln \Lambda$ due to the difference in ligand density is plotted in Fig. 8. For many of the proteins investigated, the calculated change in this quantity corresponds to an increase in the retention factor of 50–100%.

Based on these results, it was hypothesized that reproducibility of HIC data in the literature may be poor due to lot-to-lot variation in the ligand density of the resins. To test this hypothesis, isocratic elution retention factor data were compared with equivalent data in the recent literature [21,22,42]. Sample comparisons for lysozyme are plotted in Fig. 9. The trends evidenced in this sample data were consistent for all of the proteins—excellent agreement was obtained with the high-substitution phenyl resin, some discrepancy in the low-substitution phenyl data, and the butyl resin data differ substantially. Interestingly, there is disagreement in the data reported by the same group in different publications [22,32], presumably obtained with different columns; our analysis suggests that this is not a result of differences in technique or data analysis, but from variations in the stationary phase material.

Reproducibility in HIC data is critical to the effectiveness of modeling to predict the behavior of protein–resin systems for process design. Clearly, the correlations developed by Chen and Cramer [22,32] would be inaccurate in predicting the behavior of proteins on the Butyl Sepharose™ column used in this study. Further, the ligand density of materials used in high-throughput screening experiments may influence the selection of a resin for an optimized process, or affect the yield or selectivity in a process step. The model proposed in this work accounts for the ligand density both explicitly and inherently in the binary parameter ν, and may assist in explaining the poor reproducibility of the IEC data.

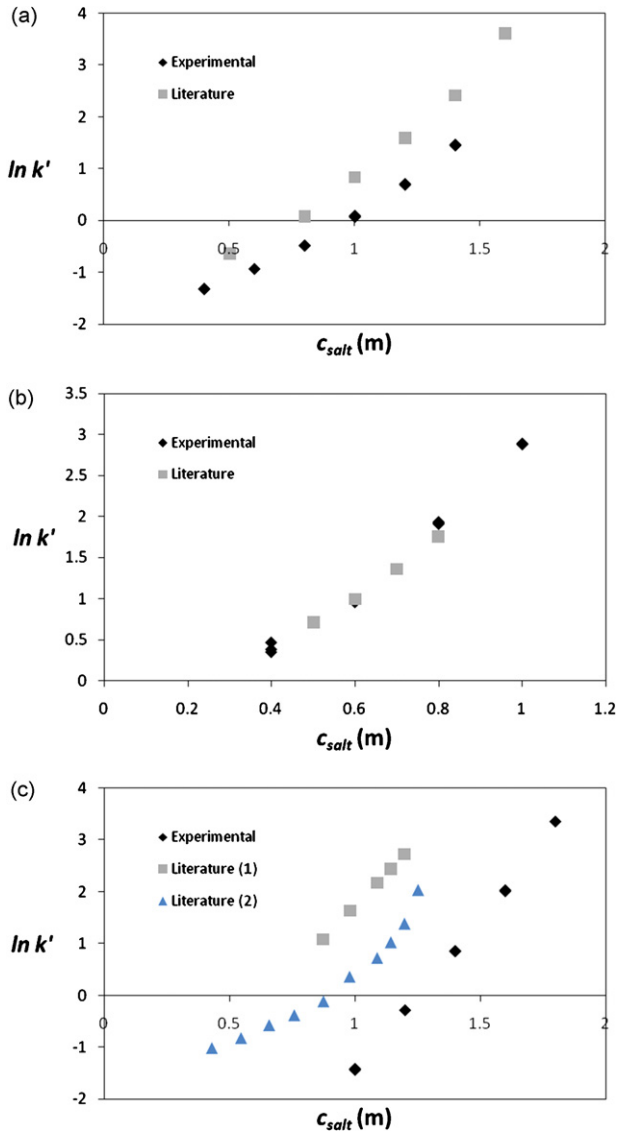

Fig. 9. Comparison of retention factor data with recent literature data for lysozyme adsorbed to (a) Phenyl Sepharose™ 6 Fast Flow (low substitution), (b) Phenyl Sepharose™ 6 Fast Flow (high substitution), and (c) Butyl Sepharose® 4 Fast Flow. Literature data are from (a, b) To and Lenhoff [21] and (c) Chen et al. [22,32].

5. Conclusion

We have presented a new thermodynamic model to describe pulse-response and non-linear loading HIC behavior in terms of the release of water molecules from hydrophobic interfaces. This model was parameterized using IEC and adsorption isotherm data for several proteins adsorbed to Sepharose™ resins of various ligand type and density. Essentially all of the data are well-described by a minimum number of parameters, and the proposed approach offers significant advantages compared to previous models and methods used for such data.

The model presented here has the potential to be used as a predictive tool to narrow the design space for HIC processes, but considerable work remains to be completed. Model parameters that are related to the salt species, protein species, and resin may be related to molecular properties in a way that will allow the estimation of how new materials or proteins will behave. To date, efforts to predict the behavior of HIC systems have largely focused on correlating protein properties, such as molecular descriptors [22,32] or hydrophobicity [46–48], with either direct measurements of protein retention or empirical parameters. These methods might be applied to the protein-dependent model parameters determined here, where the contributions of resin and protein species to the retention have been largely separated, to obtain descriptor relationships that could be applied to predict adsorption on many resins.

A large part of the protein HIC behavior is attributed to the activity of the protein in solution, characterized by the activity coefficient, in the current model. A simple linear protein activity coefficient model has been used here, that might be modified to include a Debye–Huckel term to describe behavior at low salt concentrations. Additionally, the protein activity coefficient may be related to the second osmotic virial coefficient [49] or be described by the UNIQUAC model [50,51]. To and Lenhoff have related the second osmotic virial coefficient to HIC retention factors for several proteins with some success [52]. As understanding of the solution thermodynamics of proteins increases, we expect that this will aid the application of the HIC model presented here.

Nomenclature

P_{sol}	solvated protein and associated solvent molecules
ν	stoichiometric number of ligands contacted by adsorbed protein
L	free ligand on resin surface
P_{ads}	adsorbed protein and associated ligands
ξ	stoichiometric number of water molecules released per protein–ligand contact
W	water molecule released upon adsorption
K	standard state equilibrium constant for adsorption
a_i	thermodynamic activity of species i
q_P	concentration of adsorbed protein
c_P	concentration of protein in the mobile phase
c_L	concentration of free ligand in the stationary phase
c	total concentration of species
γ_i	activity coefficient of species i
γ_i^∞	infinite dilution activity coefficient of species i in pure water
k_{salt}	incremental change in natural logarithm of solvated protein activity coefficient with change in salt concentration
c_{salt}	concentration of salt in the mobile phase
k_P	incremental change in natural logarithm of solvated protein activity coefficient with change in protein concentration
ε	empirical parameter in the relationship between adsorbed protein activity and adsorbed protein concentration
ρ	incremental change in the natural logarithm of water activity with change in salt concentration
Λ	resin ligand density
A	partition coefficient for protein adsorption
k'	chromatographic retention factor
ϕ	ratio of stationary and mobile phase volumes (phase ratio)
μ	chromatographic retention volume
V_o	elution volume of unretained species
α	salt-independent term in empirical retention factor relationship to salt concentration
β	incremental change in natural logarithm of retention factor with change in salt concentration
r_H	protein hydrodynamic radius
MW	protein molecular weight
ν_{est}	estimated number of protein–ligand contacts upon adsorption
V_s	accessible volume per volume of resin
A_s	surface area per accessible volume
$\alpha_{protein}$	empirical protein-dependent contribution to α
α_{ligand}	empirical ligand-dependent contribution to α
δ	stoichiometric number of salt molecules released upon protein adsorption
S	salt molecules released to bulk solution upon protein adsorption

References

[1] C. Saint-Hubert, A. Durieux, E. Bodo, J.P. Simon, Biotechnol. Lett. 31 (2009) 519.
[2] J.B. Lu, D. Wei, Y.F. Wang, G.Z. Wang, Biotechnol. Appl. Biochem. 52 (2009) 107.
[3] S.S. Freitas, J.A.L. Santos, D.M.F. Prazeres, Sep. Purif. Technol. 65 (2009) 95.
[4] N. Gencer, O. Arslan, J. Chromatogr. B 877 (2009) 134.
[5] J.T. McCue, P. Engel, J. Thommes, J. Chromatogr. A 1216 (2009) 902.
[6] N. Kong, X.P. Mu, H.Z. Han, W.Q. Yan, Protein Expr. Purif. 63 (2009) 134.
[7] J. Valliere-Douglass, A. Wallace, A. Balland, J. Chromatogr. A 1214 (2008) 81.
[8] A.M. Azevedo, P.A.J. Rosa, I.F. Ferreira, M.R. Aires-Barros, J. Chromatogr. A 1213 (2008) 154.
[9] J.L. Coffman, J.F. Kramarczyk, B.D. Kelley, Biotechnol. Bioeng. 100 (2008) 605.
[10] J.F. Kramarczyk, B.D. Kelley, J.L. Coffman, Biotechnol. Bioeng. 100 (2008) 707.
[11] B.F. Roettger, J.A. Myers, M.R. Ladisch, F.E. Regnier, Biotechnol. Prog. 5 (1989) 79.
[12] X.D. Geng, L. Guo, J.H. Chang, J. Chromatogr. 507 (1990) 1.
[13] F.Y. Lin, W.Y. Chen, M.T.W. Hearn, Anal. Chem. 73 (2001) 3875.
[14] C. Machold, K. Deinhofer, R. Hahn, A. Jungbauer, J. Chromatogr. A 972 (2002) 3.
[15] C. Horvath, W. Melander, I. Molnar, J. Chromatogr. 125 (1976) 129.
[16] W. Melander, C. Horvath, Arch. Biochem. Biophys. 183 (1977) 200.
[17] W.R. Melander, D. Corradini, C. Horvath, J. Chromatogr. 317 (1984) 67.
[18] J.L. Fausnaugh, F.E. Regnier, J. Chromatogr. 359 (1986) 131.
[19] T. Arakawa, S.N. Timasheff, Biochemistry 23 (1984) 5912.
[20] T.W. Perkins, D.S. Mak, T.W. Root, E.N. Lightfoot, J. Chromatogr. A 766 (1997) 1.
[21] B.C.S. To, A.M. Lenhoff, J. Chromatogr. A 1141 (2007) 191.
[22] J. Chen, T. Yang, Q. Luo, C.M. Breneman, S.M. Cramer, React. Funct. Polym. 67 (2007) 1561.
[23] J. Chen, Y. Sun, J. Chromatogr. A 992 (2003) 29.
[24] J.M. Mollerup, Fluid Phase Equilib. 241 (2006) 205.
[25] J.M. Mollerup, J. Biotechnol. 132 (2007) 187.
[26] J.M. Mollerup, T.B. Hansen, S. Kidal, A. Staby, J. Chromatogr. A 1177 (2008) 200.
[27] A. Staby, J. Mollerup, J. Chromatogr. A 734 (1996) 205.
[28] X. Geng, L. Guo, J. Chang, J. Chromatogr. 507 (1990) 1.
[29] S. Li, P. Chen, W. Li, X. Hao, G. Yang, Appl. Biochem. Biotechnol. 134 (2006) 165.
[30] K.S. Pitzer, Activity Coefficients in Electrolyte Solutions, 2nd ed., CRC Press, Boca Raton, FL, 1991.
[31] W.T. Jenkins, Protein Sci. 7 (1998) 376.
[32] J. Chen, T. Yang, S.M. Cramer, J. Chromatogr. A 1177 (2008) 207.
[33] J.L. Fogle, J.P. O'Connell, E.J. Fernandez, J. Chromatogr. A 1121 (2006) 209.
[34] Y.Z. Xiao, T.T. Jones, A.H. Laurent, J.P. O'Connell, T.M. Przybycien, E.J. Fernandez, Biotechnol. Bioeng. 96 (2007) 80.
[35] R.W. Deitcher, Y. Xiao, J.P. O'Connell, E.J. Fernandez, Biotechnol. Bioeng. 102 (2009) 1416.
[36] Y.Z. Xiao, A.S. Freed, T.T. Jones, K. Makrodimitris, J.P. O'Connell, E.J. Fernandez, Biotechnol. Bioeng. 93 (2006) 1177.
[37] B.C.S. To, A.M. Lenhoff, J. Chromatogr. A 1205 (2008) 46.
[44] R. Miller, V.B. Fainerman, A.V. Makievski, J. Kragel, D.O. Grigoriev, V.N. Kazakov, O.V. Sinyachenko, Adv. Colloid Interface Sci. 86 (2000) 39.
[45] D. Whitney, M. McCoy, N. Gordon, N. Afeyan, J. Chromatogr. A 807 (1998) 165.
[38] J.T. McCue, P. Engel, A. Ng, R. Macniven, J. Thommes, Bioprocess Biosyst. Eng. 31 (2008) 261.
[39] M.E. Lienqueo, C. Shene, J. Asenjo, J. Mol. Recognit. 22 (2009) 110.
[40] E.E.G. Rojas, J.S.D. Coimbra, L.A. Minim, S.H. Saraiva, C.A.S. da Silva, J. Chromatogr. B 840 (2006) 85.
[41] R.C.F. Bonomo, L.A. Minim, J.S.R. Coimbra, R.C.I. Fontan, L.H.M. da Silva, V.P.R. Minim, J. Chromatogr. B 844 (2006) 6.
[42] J. Chen, S.A. Cramer, J. Chromatogr. A 1165 (2007) 67.
[43] L. Hagel, in: J.C. Janson, L. Ryden (Eds.), Protein Purification, 2nd ed., John Wiley & Sons, Inc., New York, 1998, p. 79.
[46] J.C. Salgado, I. Rapaport, J.A. Asenjo, J. Chromatogr. A 1107 (2006) 110.
[47] J.C. Salgado, I. Rapaport, J.A. Asenjo, J. Chromatogr. A 1107 (2006) 120.
[48] J.C. Salgado, I. Rapaport, J.A. Asenjo, J. Chromatogr. A 1098 (2005) 44.
[49] M.L. Grant, J. Cryst. Growth 209 (2000) 130.
[50] J.A.P. Coutinho, F.L.P. Pessoas, Fluid Phase Equilib. 222 (2004) 127.
[51] S.M. Agena, I.D.L. Bogle, F.L.P. Pessoas, Biotechnol. Bioeng. 55 (1997) 65.
[52] B.C.S. To, A.M. Lenhoff, J. Chromatogr. A 1141 (2007) 235.